

# Atg26-Mediated Pexophagy Is Required for Host Invasion by the Plant Pathogenic Fungus *Colletotrichum orbiculare*

Makoto Asakura,<sup>a</sup> Sachiko Ninomiya,<sup>a</sup> Miki Sugimoto,<sup>a</sup> Masahide Oku,<sup>b</sup> Shun-ichi Yamashita,<sup>b</sup> Tetsuro Okuno,<sup>a</sup> Yasuyoshi Sakai,<sup>b,c</sup> and Yoshitaka Takano<sup>a,1</sup>

<sup>a</sup>Division of Applied Biosciences, Graduate School of Agriculture, Kyoto University, Sakyo-ku, Kyoto 606-8502, Japan

<sup>b</sup>Division of Applied Life Sciences, Graduate School of Agriculture, Kyoto University, Sakyo-ku, Kyoto 606-8502, Japan

<sup>c</sup>CREST, Japan Science and Technology Agency, 5, Chiyoda-ku, Tokyo 102-0075, Japan

The number of peroxisomes in a cell can change rapidly in response to changing environmental and physiological conditions. Pexophagy, a type of selective autophagy, is involved in peroxisome degradation, but its physiological role remains to be clarified. Here, we report that cells of the cucumber anthracnose fungus *Colletotrichum orbiculare* undergo peroxisome degradation as they infect host plants. We performed a random insertional mutagenesis screen to identify genes involved in cucumber pathogenesis by *C. orbiculare*. In this screen, we isolated a homolog of *Pichia pastoris* ATG26, which encodes a sterol glucosyltransferase that enhances pexophagy in this methylotrophic yeast. The *C. orbiculare* atg26 mutant developed appressoria but exhibited a specific defect in the subsequent host invasion step, implying a relationship between pexophagy and fungal phytopathogenicity. Consistent with this, its peroxisomes are degraded inside vacuoles, accompanied by the formation of autophagosomes during infection-related morphogenesis. The autophagic degradation of peroxisomes was significantly delayed in the appressoria of the atg26 mutant. Functional domain analysis of Atg26 suggested that both the phosphoinositide binding domain and the catalytic domain are required for pexophagy and pathogenicity. In contrast with the atg26 mutant, which is able to form appressoria, the atg8 mutant, which is defective in the entire autophagic pathway, cannot form normal appressoria in the earlier steps of morphogenesis. These results indicate a specific function for Atg26-enhanced pexophagy during host invasion by *C. orbiculare*.

## INTRODUCTION

Peroxisomes are single-membrane-bound organelles that are conserved between lower and higher eukaryotes and conduct various lipid metabolism and hydrogen peroxide detoxification functions. They are also required for specific functions, such as methanol assimilation in the yeast *Pichia pastoris* (Subramani, 1993). The number of peroxisomes can increase or decrease dramatically in response to various environmental cues. For example, yeast peroxisomes proliferate in response to nutritional stimuli, such as oleate and methanol, to metabolize these substrates (Gurvitz and Rottensteiner, 2006). In mammals, it is well known that peroxisome proliferators increase peroxisomal activity and abundance (Desvergne and Wahli, 1999). It has recently been shown that light induces the proliferation of peroxisomes in *Arabidopsis thaliana* (Desai and Hu, 2008).

In general, organelle homeostasis is maintained by balancing their synthesis and degradation. Peroxisomal biosynthesis re-

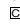
quires a group of well-conserved peroxin proteins, the products of *PEX* genes (Eckert and Erdmann, 2003). Mutations of the *PEX* genes not only abolish peroxisome assembly but also result in various disorders at higher levels of biological function, including Zellweger syndrome in humans, embryo lethality in the model plant *Arabidopsis*, and the loss of phytopathogenicity in some plant pathogens (Kimura et al., 2001; Fan et al., 2005; Fujiki et al., 2006; Ramos-Pamplona and Naqvi, 2006).

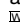
Peroxisomes are degraded by a type of selective autophagy, called pexophagy, which is conserved from yeasts to humans (Farré and Subramani, 2004; Sakai et al., 2006). In *P. pastoris*, growth on methanol as the sole carbon source induces peroxisome proliferation, but changing the carbon source to glucose or ethanol promotes the degradation of peroxisomes via pexophagy. Recent studies have shown that many of the ATG (for autophagy-related) gene products necessary for nonselective autophagy, such as Atg8, are also necessary for pexophagy (Stromhaug et al., 2001; Mukaiyama et al., 2002) and that a subset of several genes, for example, ATG26 and ATG30, are preferentially required for pexophagy (Oku et al., 2003; Farré et al., 2008).

Asexual spores, called conidia, of many phytopathogenic fungi germinate and develop specific infection structures called appressoria, which are capable of invading host plants (infection-related morphogenesis). *Colletotrichum orbiculare* (syn. *C. lagenarium*), the causal agent of cucumber anthracnose, forms appressoria that are darkly pigmented with melanin (Agrios, 2004). Melanin is a secondary metabolite that is essential for the function of the appressoria, and inhibitors of melanin

<sup>1</sup> Address correspondence to ytakano@kais.kyoto-u.ac.jp.

The author responsible for distribution of materials integral to the findings presented in this article in accordance with the policy described in the Instructions for Authors (www.plantcell.org) is: Yasuyoshi Sakai (ysakai@kais.kyoyo-u.ac.jp) and Yoshitaka Takano (ytakano@kais.kyoto-u.ac.jp).

 Some figures in this article are displayed in color online but in black and white in the print edition.

 Online version contains Web-only data.

www.plantcell.org/cgi/doi/10.1105/tpc.108.060996

biosynthesis, such as tricyclazole and carpropamid, are widely used as effective chemicals to protect plants from fungal diseases (Kubo and Furusawa, 1991).

The *C. orbiculare* peroxin Pex6 (previously named ClaPex6) has been identified as an essential factor for fungal pathogenicity in *C. orbiculare* (Kimura et al., 2001). The *pex6* mutant of *C. orbiculare* forms nonfunctional appressoria with severely reduced melanization, indicating that peroxisomal functions are required for appressorium maturation and function. Pex6 is also required for the pathogenicity of the rice blast fungus *Magnaporthe oryzae*, and the Mo *pex6* mutant displays a defect in appressorial melanization, indicating common functions for the peroxisomes in fungal pathogenesis (Ramos-Pamplona and Naqvi, 2006; Wang et al., 2007). Recently, the inhibition of the entire autophagic pathway was reported to cause the loss of phytopathogenicity of *M. oryzae* (Veneault-Fourrey et al., 2006; Liu et al., 2007). However, peroxisome degradation and its relationship to pathogenicity have not been studied in plant pathogenic fungi.

In previous studies, we and others have identified *ATG26* as a factor that activates pexophagy in the yeast *P. pastoris* (Oku et al., 2003; Nazarko et al., 2007b). Pp *ATG26* encodes a sterol glucosyltransferase that is required for ergosterol glucoside biosynthesis (UDP-glucose:sterol glucosyltransferase, EC 2.4.1.173) and contains a phosphoinositide binding domain (PBD). Pp *Atg26* is recruited to a cytosolic protein–lipid nucleation complex through its PBD and activates the elongation and maturation of an autophagosome-like structure (Yamashita et al., 2006). Domain analyses of Pp *Atg26* have indicated that the catalytic subunit of Pp *Atg26*, without the PBD, is not sufficient for pexophagy function and that the catalytic ergosterol synthesis reaction at the protein–lipid nucleation complex is critical for pexophagy.

However, the Pp *atg26* knockout mutant showed no obvious phenotypic defects other than in pexophagy (Oku et al., 2003). Hence, the physiological role of pexophagy was not identified. In this report, the *C. orbiculare* *Atg26* ortholog (Co *Atg26*) is identified as a factor required for pathogenicity and the development of cucumber anthracnose symptoms. An intimate relationship between pexophagy and fungal pathogenicity is suggested, and the consistently abundant peroxisomes seen in the conidia before the start of morphogenesis are degraded during infection-related morphogenesis. In contrast with the *C. orbiculare* *pex6* mutant, which is defective in appressorial melanization, the *atg26* mutant can develop melanized appressoria but exhibits a defect in the subsequent invasion step. Further studies have revealed that Co *Atg26* is involved in the regulation of peroxisome homeostasis in the appressoria, indicating the physiological significance of pexophagy in the invasion of the host plant by this fungus.

## RESULTS

### *ATG26* Is Required for Full Virulence of *C. orbiculare*

To identify the genes responsible for the pathogenicity of *C. orbiculare*, a random insertional mutant library of *C. orbiculare*

generated by restriction enzyme–mediated integration (REMI) was screened for mutants that were defective in pathogenicity on host cucumber leaves. Of these, the mutant NP71 exhibited a significant reduction in pathogenicity on cucumber leaves (see Supplemental Figure 1 online). The REMI-introduced plasmid was determined to be integrated into an open reading frame (ORF) encoding a protein of 1475 amino acids (Figure 1A; see Supplemental Figure 2 online). The deduced amino acid sequence of the tagged ORF exhibited high similarity to that of *Atg26* of various yeasts, for example, Pp *Atg26* of *P. pastoris* and Sc *Atg26* of *Saccharomyces cerevisiae*, and those of the filamentous fungi (see Supplemental Figure 2 online). This *ATG26* homolog of *C. orbiculare* was designated Co *ATG26*.

We next generated a Co *ATG26* insertional mutant by introducing the disruption vector pKOATG26 into the wild-type strain (see Supplemental Figure 3 online). The resulting Co *atg26* strain exhibited slightly slower growth on potato dextrose agar (PDA) medium compared with that of the wild-type strain (see Supplemental Table 1 online). The conidiation of the *atg26* strain was reduced to ~16% relative to that of the wild-type strain (see Supplemental Table 1 online). The *atg26* strain exhibited significantly reduced pathogenicity on cucumber cotyledons (Figure 1B) but occasionally formed faint lesions. Also, the *pex6* mutant, which is defective in peroxisome biogenesis, failed to form lesions in the same inoculation assays (Figure 1B). The reintroduction of the Co *ATG26* DNA into the *atg26* strain complemented the pathogenic defect of the mutant (Figure 1B). From these results, we conclude that *ATG26* is critical for pathogenicity of *C. orbiculare*. We previously reported that pathogenicity of the *pex6* mutant was partially restored by addition of glucose (Kimura et al., 2001). By contrast, addition of glucose did not restore pathogenicity of the *atg26* mutant (see Supplemental Figure 4 online).

An inoculation assay through wounds indicated that *ATG26* is not essential for necrotrophic invasive growth inside the host plant tissue at the postinvasion stage (Figure 1C). The infection-related morphogenesis of the *atg26* strain was investigated on both glass and host plant surfaces. Germ tubes of the *atg26* strain differentiated into appressoria that were pigmented with melanin (Figures 1D and 2A). This is distinct from the *pex6* mutant, which forms colorless appressoria. These findings suggest that the *atg26* strain has a defect in the host-invasion step via the appressoria.

### The *atg26* Mutant Shows a Specific Defect in Host Invasion

To assess appressorial functionality, we performed a penetration assay on the host cucumber plant. More than 35% of the appressoria of the wild-type strain formed infectious hyphae, which invaded the host plant tissue 4 d after inoculation. By contrast, the Co *atg26* strain formed few infectious hyphae (Figures 2A and 2B). During host invasion, *C. orbiculare* initially establishes a biotrophic interaction via the formation of intracellular hyphae, which are surrounded by the plant membrane (Perfect et al., 1999). In the *M. oryzae*–rice interaction, the intracellular hyphae are sealed by a plant membrane called the extrainvasive hyphal membrane (EIHM), which can be labeled with the endocytotic tracker FM4-64 (Kankanala et al., 2007). To assess the host invasion–associated defect in the *atg26* mutant

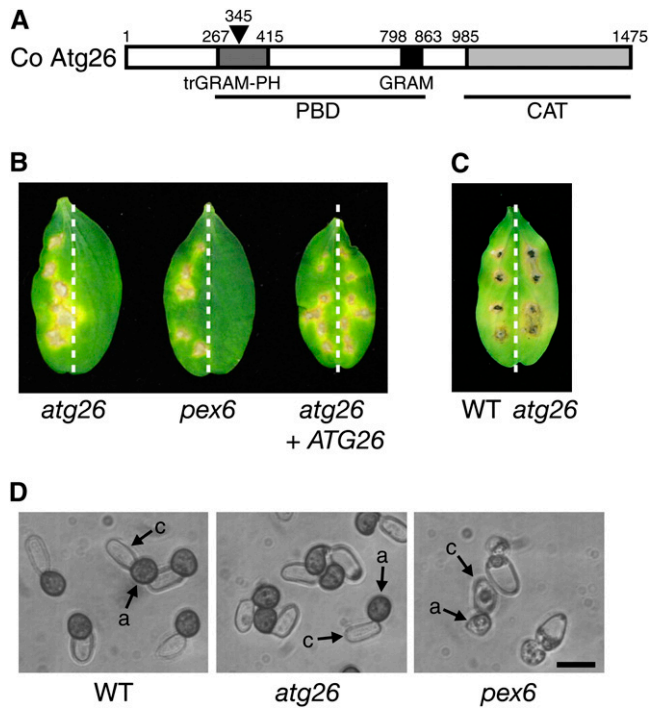


**Figure 1.** *ATG26* Is a Factor Required for the Fungal Pathogenicity of *C. orbiculare*.

(A) Schematic drawing of the annotated domains within *Atg26* of *C. orbiculare*. Co *Atg26* has a PBD and a catalytic domain (CAT). The PBD comprises glucosyltransferases, Rab-like GTPase activators, a myotubularins (GRAM) domain, and a truncated GRAM (trGRAM)–pleckstrin homology (PH) domain. The insertion site of the *HPH* cassette into Co *ATG26* in the knockout mutants is indicated by an arrowhead. The numbers indicate amino acid residues.

(B) Pathogenicity assays on the host plant. On the left halves of the cucumber cotyledons, the wild-type strain 104-T was inoculated as the positive control. The tested strains were inoculated on the right halves. Inoculated leaves were incubated for 7 d.

(C) Assay for invasive growth of the *atg26* mutant in the postinvasion stage. Mycelial blocks of the tested strains were inoculated onto the wound sites of cucumber cotyledons. On the left halves of the cotyledons, 104-T was inoculated as the positive control. On the right halves, the *atg26* strain was inoculated. The inoculated plants were incubated for 7 d.

(D) Appressorium formation in the *atg26* knockout mutant. Conidial suspensions of each strain were incubated on glass for 12 h. a, appressorium; c, conidium. Bar = 10  $\mu$ m.

[See online article for color version of this figure.]

In detail, we investigated the biotrophic interaction of the *atg26* mutant using epidermal cells of cucumber cotyledons. We concomitantly labeled *C. orbiculare* and the putative EIHM with green fluorescent protein (GFP) or FM4-64 (red), respectively. We tried to find a rare invasion site of the *atg26* mutant and investigated the dynamics of plant membranes at that site. The invasive hyphae of the *atg26* mutant, labeled with GFP, were sealed by FM4-64-labeled plant membranes of the epidermal cells, indicating that the *atg26* mutant retains the ability to form intracellular hyphae at the biotrophic stage (Figure 2C). These

results indicate that *ATG26* is specifically required for appressorial functionality in host invasion.

### Autophagic Degradation of Peroxisomes during Infection-Related Morphogenesis

After confirming the involvement of *ATG26* in the pathogenicity of *C. orbiculare*, we hypothesized that the efficient peroxisome

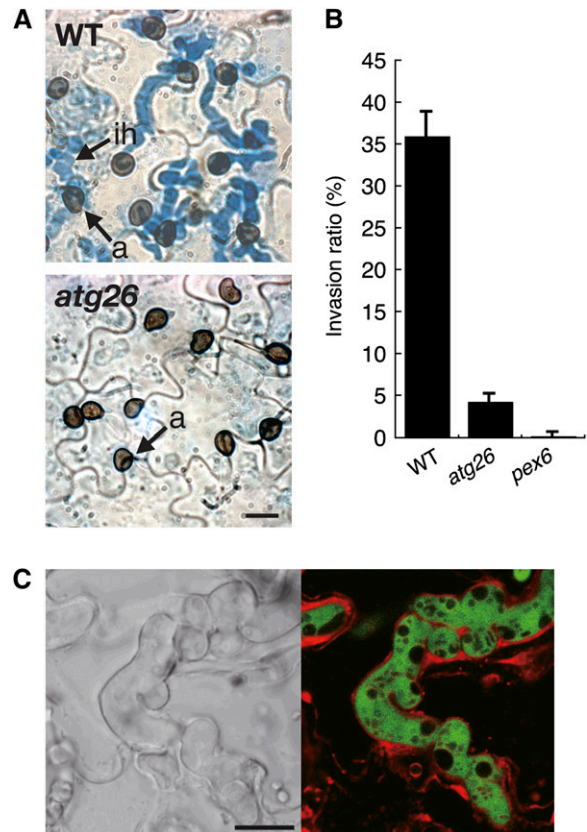


**Figure 2.** The *atg26* Mutant Is Defective in Appressorium-Mediated Host Invasion.

(A) The *atg26* mutant failed to effectively form invasive hyphae. A conidial suspension of each strain was inoculated onto the lower surfaces of cucumber cotyledons and incubated for 4 d. The invasive hyphae were stained with lactophenol aniline blue. a, appressorium; ih, invasive hypha. Bar = 10  $\mu$ m.

(B) Quantitative assay for appressorium-mediated host invasion. Conidial suspensions of each strain were inoculated onto the lower surfaces of cucumber cotyledons, and the cotyledons were incubated for 4 d. The proportion of appressoria forming invasive hyphae was calculated as follows. In each experiment, at least 100 appressoria were examined and counted to calculate the percentage of invasive hyphae. The means and standard deviations were calculated from three independent experiments.

(C) Invasive hyphae of the *atg26* mutant were sealed by membrane in the invaded cells of cucumber cotyledons. The *atg26* mutant expressing GFP was inoculated onto the lower surfaces of cucumber cotyledons. At 4 d after inoculation, the epidermis of the inoculated plants was peeled off and stained with FM4-64 for 30 min. Bar = 10  $\mu$ m.

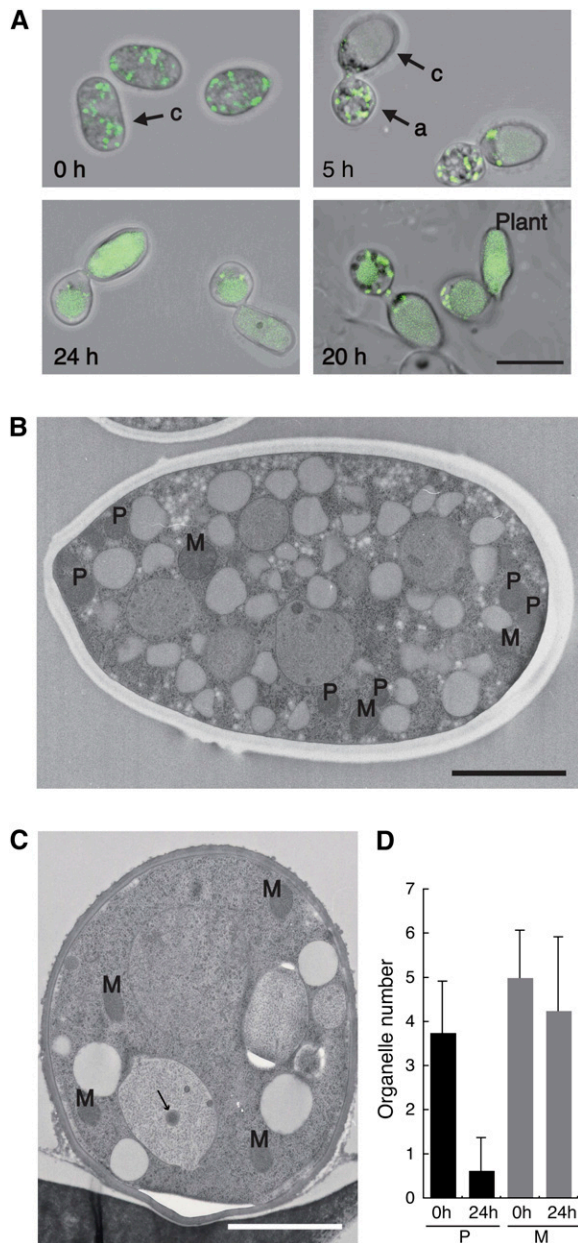


**Figure 3.** Degradation of Peroxisomes during the Infection-Related Morphogenesis of *C. orbiculare*.

**(A)** Peroxisome degradation during the appressorium formation process. Conidia from the wild-type strain expressing GFP-SKL were incubated either on glass or on cucumber tissue (plant). Merged differential interference contrast and GFP fluorescence images are shown. a, appressorium; c, conidium. Bar = 10  $\mu$ m.

**(B)** Transmission electron micrograph of a conidium. In a preincubated conidium, abundant peroxisomes (P) and mitochondria (M) were observed. Bar = 2  $\mu$ m.

**(C)** Transmission electron micrographs of an appressorium. By contrast, the number of peroxisomes was markedly reduced in an appressorium. An arrow indicates a putative peroxisome inside a vacuole. Bar = 2  $\mu$ m.

**(D)** Preferential degradation of peroxisomes in appressoria. The numbers of peroxisomes (P) and mitochondria (M) in preincubated conidia (0 h)

degradation mediated by Atg26 is required for fungal pathogenicity. To assess this hypothesis, we first examined whether peroxisomes are degraded in vacuoles during the infection-related morphogenesis of *C. orbiculare*. When GFP-tagged peroxisomal targeting signal 1 (GFP, the tripeptide SKL) was expressed in the conidia of the wild type, abundant fluorescent dots representing peroxisomes were observed (Figure 3A). After 5 h of incubation, a germ tube emerged from the conidium and differentiated into a swollen appressorium. At the same time, vacuoles formed inside the conidium. At this time point, abundant fluorescent dots representing peroxisomes were observed in the nascent appressoria, together with a gradual reduction in peroxisomal dots in the conidia and the diffusion of GFP fluorescence. At 24 h, when appressoria had matured for the subsequent invasion process, diffuse GFP fluorescence was observed in the appressoria instead of the GFP dots (Figure 3A), suggesting peroxisome degradation in the infection structure. The diffuse fluorescence subsequently became weaker as the incubation proceeded (data not shown). Similar results were also observed on the surface of the host plants (Figure 3A, bottom right panel). To confirm the degradation of the peroxisomes in the appressorial cells, we investigated the peroxisome dynamics in single appressoria by time-lapse analysis using fluorescence microscopy and observed the degradation of peroxisomes labeled with GFP-SKL (see Supplemental Figure 5 online).

We also used thin-section electron microscopy to investigate the status of peroxisome size and populations in *C. orbiculare*. In the preincubated conidia of *C. orbiculare*, several peroxisomes were observed, and the sizes of all the peroxisomes were almost uniform (Figure 3B). After 24 h of incubation, the number of peroxisomes was significantly reduced (Figures 3C and 3D). In contrast with peroxisomes, the number of mitochondria was not markedly reduced in the appressoria (Figures 3B to 3D). These data suggest that peroxisomes are preferentially degraded during the infection-related morphogenesis of *C. orbiculare*.

To study the features of peroxisome degradation in detail, we simultaneously labeled the peroxisomes with red fluorescent protein (RFP)-SKL and the vacuoles with Oregon Green 488 carboxylic acid diacetate (cDFFDA; Hicky et al., 2004). After incubation for 5 h, diffuse RFP-SKL fluorescence was detected inside the conidia vacuoles labeled with cDFFDA (Figure 4A, top panels). At 16 h, diffuse RFP fluorescence was detected inside the appressoria vacuoles (Figure 4A, bottom panels).

When the peroxisomes are degraded via the autophagic process, they are first sequestered by autophagosomal membranes and then delivered to vacuoles. Atg8 localizes at the autophagosomal membranes during the autophagic process; therefore, GFP-Atg8 can be used as a general marker for autophagy (Klionsky and Ohsumi, 1999; Ohsumi, 2001). We isolated the ortholog of *ATG8* from *C. orbiculare* (Co *ATG8*) and constructed a *GFP-CoATG8* fusion gene. Functional GFP-CoAtg8 and RFP-SKL were coexpressed to monitor the

and appressoria (24 h) were counted. Each mean and standard deviation was calculated from eight transmission electron microscopy (TEM) sections.

[See online article for color version of this figure.]

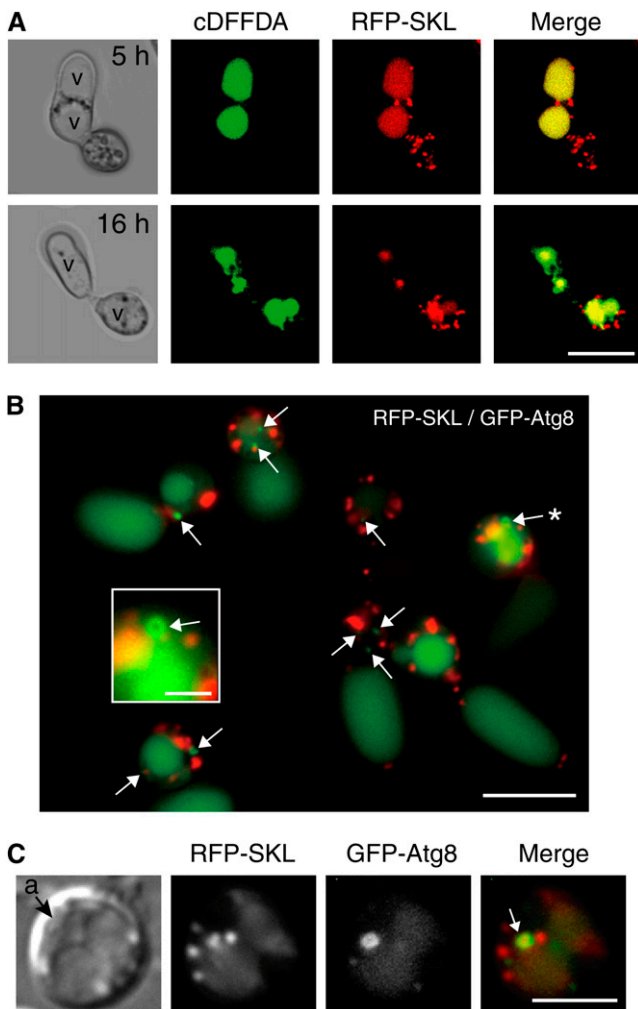


**Figure 4.** Autophagic Degradation of Peroxisomes inside Vacuoles.

**(A)** Conidia from the wild-type strain expressing RFP-SKL were incubated on glass for 5 or 16 h and then stained with cDFFDA to visualize the vacuoles. v, vacuole. Bar = 10  $\mu\text{m}$ .

**(B)** Atg8-localizing autophagosomes during appressorial maturation. Functional GFP-CoAtg8 was coexpressed with RFP-SKL in the *atg8* mutant. GFP-CoAtg8 dots representing putative autophagosomal structures (indicated by arrows) were detected after 13 h of incubation. A ring structure labeled by GFP-CoAtg8 is indicated by an asterisk. Bar = 10  $\mu\text{m}$ . Magnified image of the ring structure is also shown inside the white box (bar = 2  $\mu\text{m}$ ).

**(C)** Engulfment of peroxisomes by autophagosomes labeled with GFP-CoAtg8. A differential interference contrast micrograph is shown in the left panel. A merged image of RFP-SKL (peroxisomal matrix, red) and GFP-CoAtg8 (green) is shown in the right panel. Bar = 5  $\mu\text{m}$ .

dynamics of the autophagosomes and peroxisomes in the appressoria of *C. orbiculare*. Fluorescent dots of GFP-CoAtg8, representing autophagosomes, were frequently detected inside the appressoria at 12 to 16 h. We also detected ring structures labeled with GFP-CoAtg8 (Figure 4B). Dots of GFP-CoAtg8 were frequently associated with RFP-SKL signals, representing per-

oxisomes (Figure 4B), and the GFP-labeled autophagosomes were also observed to incorporate the RFP-labeled peroxisomes, showing the selective autophagy of the peroxisomes, which is pexophagy (Figure 4C). We also observed diffusion of GFP-CoAtg8 fluorescence in the vacuolar lumen of conidia (Figure 4B). This may be due to the occurrence of extensive nonselective macroautophagy during earlier infection phase (see below).

#### Atg26-Enhanced Pexophagy in the Fungal Infection Structure

Previous studies have shown that the extent of the contribution of Atg26 to pexophagy depends on the species and/or the medium applied to induce pexophagy (Oku et al., 2003; Cao and Klionsky, 2007; Nazarko et al., 2007b). We assessed the extent of Co Atg26 involvement in pexophagy during the infection-related morphogenesis of *C. orbiculare*. We first examined peroxisome biogenesis in the Co *atg26* mutant. When GFP-SKL was expressed in the *atg26* strain, we found abundant punctate fluorescence conidia, as observed in conidia of the wild-type strain, demonstrating normal peroxisome biogenesis in the absence of Atg26 (Figure 5A). Conversely, no punctate fluorescence was detected in the conidia of the *pex6* mutant expressing GFP-SKL (Figure 5A).

Next, we followed pexophagy in the *atg26* strain and the wild-type strain. At 2.5 h of incubation when conidia produced germ tubes, both strains exhibited abundant fluorescent dots representing peroxisomes (see Supplemental Figure 6 online). At 3.5 h of incubation when germ tubes were differentiating appressoria, peroxisomes of both strains were degraded in the conidia but not in the appressoria (see Supplemental Figure 6 online). After incubation for 24 h, the fluorescent dots of GFP-SKL became scarce in the mature appressoria of the wild-type strain (Figures 3A and 5B). By contrast, bright peroxisomal dots were maintained in the appressoria of the *atg26* strain (Figure 5B). Quantitative analysis revealed that the amount of remaining peroxisomes was significantly higher in the *atg26* mutant (Figure 5C). Further biochemical analysis on pexophagy was hindered by difficulties in collecting the appressoria during infection-related morphogenesis and lack of the specific antibodies against proper peroxisomal proteins. Involvement of Atg26 in the yeast Cvt (cytoplasm to vacuole targeting) pathway was also reported (Nazarko et al., 2007a). However, neither the Cvt pathway nor Ape1 homolog (the specific cargo for the Cvt pathway) has been identified with this fungus. Therefore, we concluded that the efficiency of pexophagy in the appressoria of the *atg26* strain was significantly reduced compared with that in the wild-type strain.

We also generated the *atg26* null mutant (*atg26 $\Delta$* ), in which the entire ORF of *ATG26* was deleted in the background of the wild-type strain expressing GFP-SKL. The generated *atg26 $\Delta$*  strain exhibited a phenotype identical to that of the *atg26* insertional strain in all tested aspects, including growth, conidiation, pathogenicity, and pexophagy (see Supplemental Table 1 and Supplemental Figure 7 online). These data confirm the complete inactivation of Atg26 in the *atg26* strain.

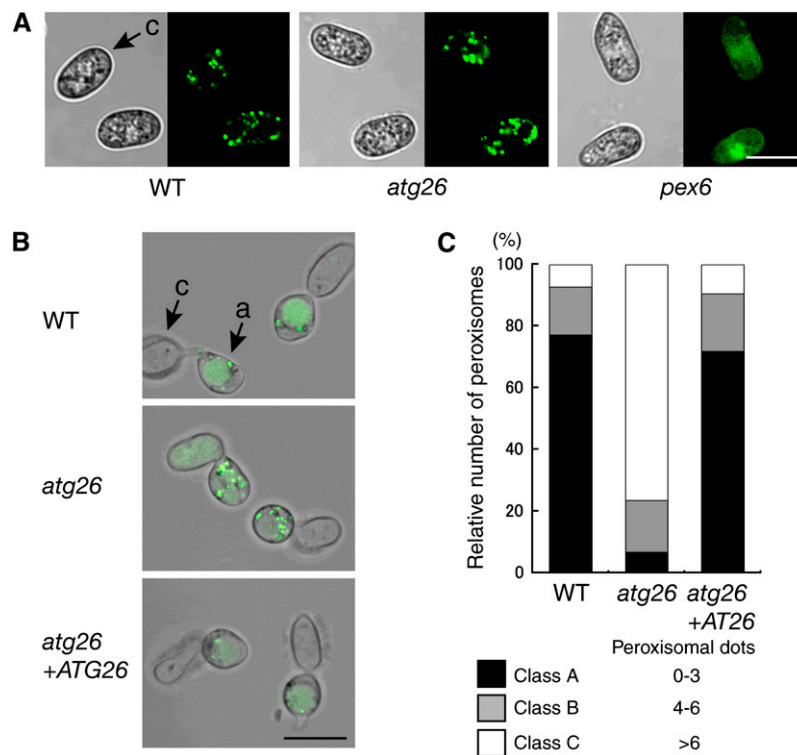


**Figure 5.** Atg26-Dependent Pexophagy and Fungal Pathogenesis.

**(A)** Peroxisome assembly in the *atg26* mutant. GFP-SKL was expressed in tested strains, and the GFP fluorescence was observed in the conidia. Bar = 10  $\mu$ m. c, conidium.

**(B)** The *atg26* mutant exhibits a defect in pexophagy. Conidia from the tested strains expressing GFP-SKL were incubated on glass for 24 h. Bar = 10  $\mu$ m. a, appressorium; c, conidium.

**(C)** Quantitative analysis of pexophagy in appressoria. Conidia from the tested strains expressing GFP-SKL were incubated on glass for 24 h. For each experiment, punctate dots of GFP fluorescence representing peroxisomes were counted in the appressoria ( $n = 100$ ) and the values were divided into three classes (class A, zero to three punctate dots; class B, four to six punctate dots; class C, more than six punctate dots). The percentage of each class in the tested strains was calculated. Data represent the means from three independent experiments that gave similar results.

[See online article for color version of this figure.]

### Both the Phosphoinositide Binding and Catalytic Domains of Atg26 Are Required for Infection-Related Pexophagy

Previously, sterol glucoside synthesized by the protein Chip6 was reported to be involved in the pathogenicity of *Colletotrichum gloeosporioides* on avocado fruit (Kim et al., 2002). Unlike Chip6, Atg26 has a PBD in addition to its catalytic domain (CAT) (Figure 6A). Our previous study using methanol-induced *P. pastoris* cells demonstrated that the enhancement of pexophagy required both the CAT and PBD (Oku et al., 2003). Sterol glucoside synthesis, by contrast, requires only the CAT (Oku et al., 2003). To confirm the relationship between pexophagy and phytopathogenicity at the molecular level, we conducted domain-deletion analysis of Co ATG26. In addition to full-length ATG26 (ATG26FL), we generated the following ATG26 variants: ATG26 lacking the CAT region (ATG26 $\Delta$ CAT), ATG26 lacking the PBD region (ATG26 $\Delta$ PBD), and ATG26 with only the CAT region (ATG26CAT) (Figure 6A). These constructs were introduced into the *atg26* strain expressing GFP-SKL. The introduction of ATG26FL into the *atg26* strain rescued fungal pathogenicity

(Figure 6B). Analysis of pexophagy based on GFP-SKL also revealed that the introduction of ATG26FL rescued pexophagy in the *atg26* strain (Figure 6B). By contrast, ATG26 $\Delta$ CAT failed to rescue the pexophagy defect in the *atg26* strain and did not restore its pathogenicity (Figure 6B). These results show that the catalytic region of Atg26 is essential for both pexophagy and pathogenicity (Figure 6B).

ATG26 $\Delta$ PBD did not restore the defects in pexophagy and pathogenicity in the *atg26* strain. ATG26CAT also failed to rescue the defects of this strain, suggesting the importance of the PBD in Atg26 (Figure 6B). We measured the activity of sterolglucosyl transferase(s) in the wild-type and three mutant strains: (1) the *atg26* strain, (2) the *atg26* strain with ATG26FL, and (3) the *atg26* strain with ATG26 $\Delta$ PBD (Figure 6C). Sterolglucosyl transferase activity was clearly detected in the *atg26* strain and in the wild-type strain, although the activity in the *atg26* strain was lower than that in the wild-type strain. These results suggest that Atg26 does indeed have sterolglucosyl transferase activity, although additional sterolglucosyl transferase(s) is also present in *C. orbiculare*. Whereas the introduction of ATG26 $\Delta$ PBD and ATG26FL elevated

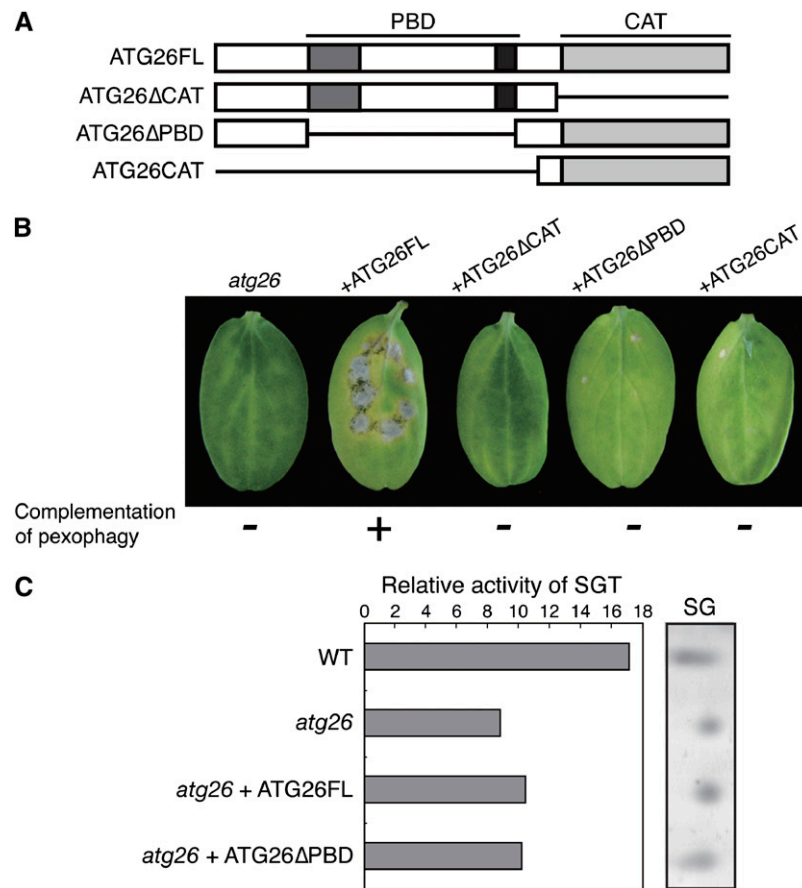


**Figure 6.** Functional Domain Analysis of Atg26.

**(A)** Deletion constructs of Co Atg26 used for domain analysis. Full-length ATG26 (ATG26FL), ATG26 lacking the catalytic domain (ATG26ΔCAT), ATG26 lacking the PBD (ATG26ΔPBD), or the ATG26 catalytic domain (ATG26CAT) were introduced into the *atg26* strain expressing GFP-SKL.

**(B)** Pathogenicity and pexophagy of the strains transformed with each construct. Each transformant was inoculated onto cucumber cotyledons and the inoculated plants were incubated for 1 week. The pexophagy of each transformant was also assayed. The introduction of ATG26FL complemented the defects in the pathogenicity and pexophagy of the *atg26* mutant.

**(C)** Sterol glucosyltransferase (SGT) assay. Particulate fractions from the cell homogenates of the tested strains were incubated with cholesterol and UDP-glucose to estimate the sterol glucoside (SG) synthesis activity. Lipids were extracted from mixed samples, separated by thin-layer chromatography, and exposed to methylresorcinol to detect the glycolipids. The relative SGT activity was determined using Metamorph version 6.0 (Nihon Molecular Devices) from one out of two independent experiments that gave similar results.

[See online article for color version of this figure.]

the sterolglucosyl transferase activity in the *atg26* strain (Figure 6C), ATG26ΔPBD failed to rescue the defects in both pexophagy and pathogenicity in this strain (Figure 6B). These results suggest that the sterolglucosyl transferase activity of Atg26 is alone insufficient for the functional pexophagy and pathogenicity in *C. orbiculare* and that an additional function of the PBD in Atg26 is required for both pexophagy and pathogenicity.

The PBD is necessary for the recruitment of Pp Atg26 to the preautophagosomal structure during pexophagy in *P. pastoris* (Oku et al., 2003; Yamashita et al., 2006). We investigated the intracellular localization of both Co Atg26 (ATG26) and Co Atg26 lacking the PBD (ATG26ΔPBD) by the expression of each protein fused to GFP (Figure 7A). GFP fused to full-length Atg26 (GFP-ATG26FL) restored the pathogenicity of the *atg26* mutant, but

GFP fused to Atg26, lacking the PBD (GFP-ATG26ΔPBD), failed to restore it (Figure 7B). In transformants carrying GFP-ATG26FL, we observed fluorescent GFP dots that probably represent preautophagosomal structures (Figure 7C). By contrast, in transformants carrying GFP-ATG26ΔPBD, no such fluorescent dots were observed, suggesting that the PBD of Atg26 is required for the proper intracellular recruitment of Atg26 to membrane structures for pexophagy (Figure 7C).

#### Involvement of Nonselective Autophagy in Fungal Morphogenesis during the Early Infection Period

Atg26 was not essential for nonselective autophagy in all the yeast species tested (Oku et al., 2003; Cao and Klionsky, 2007;

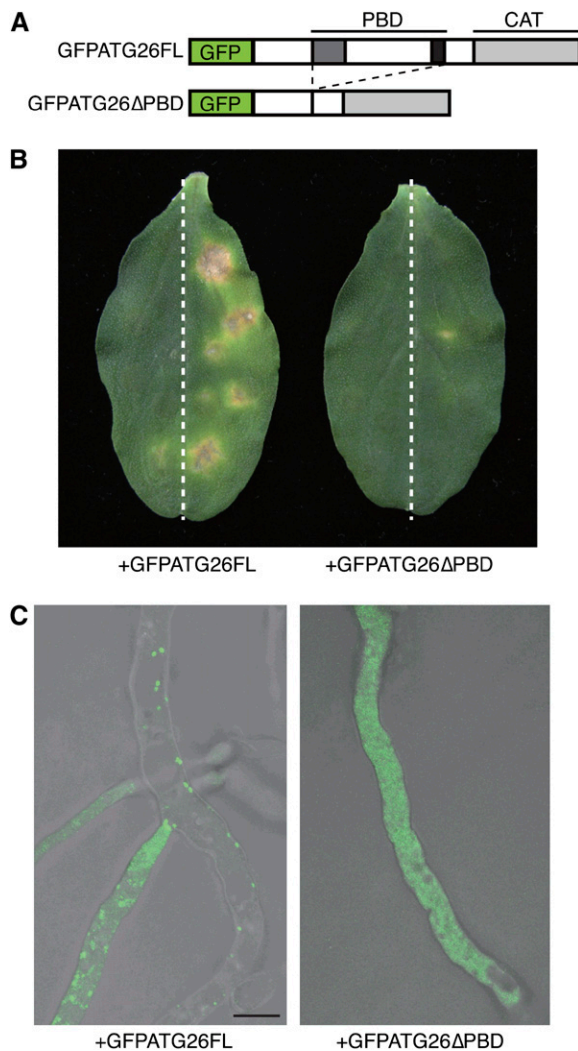


**Figure 7.** PBD-Dependent Localization of Atg26 in the Putative Preautophagosome Structure.

**(A)** Constructs for the GFP-based localization analysis of Co Atg26.  
**(B)** Introduction of GFP-Atg26 but not of GFP-Atg26 lacking PBD restored the pathogenicity of the *atg26* strain. Each transformant was inoculated onto the right half of a cucumber cotyledon and incubated for 1 week. The *atg26* mutant was inoculated onto the left half of each cotyledon.  
**(C)** Intracellular localization of GFP-CoAtg26. Mycelial cells of each transformant were observed by confocal microscopy. Bar = 10  $\mu\text{m}$ .  
 [See online article for color version of this figure.]

Nazarko et al., 2007b). To understand the role of autophagy in a more general context, we cloned the *ATG8* homolog (designated Co *ATG8*) from *C. orbiculare*. We generated a Co *ATG8*-disrupted strain in *C. orbiculare* (see Supplemental Figure 8 online). This *atg8* mutant exhibited slightly reduced growth on nutrient-rich medium (PDA), and it also displayed a severe reduction in conidiation (Figure 8A; see Supplemental Table 1 online). An inoculation assay showed the loss of pathogenicity in the *atg8* mutant on cucumber cotyledons, indicating that *ATG8*

is required for the fungal pathogenicity of *C. orbiculare* (Figure 8B).

The infection behavior of the *atg8* mutant was investigated by microscopy. The conidia of the *atg8* mutant exhibited severe germination defects on a glass surface (Figure 8C). Approximately 50% of the conidia of the mutant failed to germinate on glass (Figure 8D). The germinating conidia of the mutant also exhibited a defect in appressorial development (Figures 8C and 8D). These results show that the *atg8* mutant is defective in the early stages of infection-related morphogenesis, such as in germination, which is distinct from the *atg26* mutant, which is defective in host invasion. A penetration assay also showed that the appressoria formed by the *atg8* strain were nonfunctional (Figure 8E). When RFP was expressed in the cytosol of the *atg8* strain, RFP fluorescence was observed exclusively in the cytoplasm, not in the vacuolar lumen, indicating a critical role for Atg8 in nonselective macroautophagy during appressorial development (Figure 8F). By contrast, RFP fluorescence was detected strongly inside the vacuoles of the *atg26* mutant, suggesting efficient nonselective autophagy in this strain (Figure 8F). Consistently, nitrogen starvation treatment induced accumulation of cytosolic RFP to the vacuoles of mycelia in the *atg26* mutant but not in the *atg8* strain (see Supplemental Figure 9 online). Considering together all the phenotypic differences between the *atg8* and *atg26* mutants during the infection period, Atg8-mediated nonselective autophagy appears to be required for the early stage of infection-related morphogenesis. By contrast, the efficient pexophagy enhanced by Atg26 is specifically required for the subsequent host-invasion step.

#### Atg26-Mediated Pexophagy and Appressorial Functionality

To further understand the physiological functions of Co Atg26-mediated pexophagy, we performed a detailed phenotypic analysis of the *atg26* mutant in terms of appressorial functionality.

It has been reported that mutants of *C. orbiculare* defective in penetration peg formation failed to induce papillae on the non-host plant *Arabidopsis* (Shimada et al., 2006). We found that the appressoria of the *atg26* mutant elicited papilla formation on *Arabidopsis*, suggesting that the *atg26* mutant retains the ability to develop a penetration peg (Figure 9A). Consistent with this, the *atg26* mutant penetrated the artificial nitrocellulose membranes, as did the wild-type strain (Figure 9B).

To test a possibility that host defense responses play a role in the failure of the *atg26* mutant to invade host epidermal cells, we also investigated the pathogenicity of the *atg26* mutant on host plants whose defense responses were partially compromised by heat treatment. Cucumber plants were heat shocked and then inoculated with 104-T, the *atg26* mutant, or *pex6* mutant. After incubation for 7 d, the *atg26* mutant formed lesions on the heat-shocked cucumber cotyledons (Figure 9C). By contrast, the *pex6* mutant failed to form lesions (Figure 9C). These data suggest that host defense responses are involved in the failure of the *atg26* mutant in host invasion.

In *Magnaporthe* and *Colletotrichum* species, appressoria produce the internal turgor pressure that is required to develop a penetration peg into the host epidermal cell (Howard et al., 1991; de Jong et al., 1997; Bechinger et al., 1999). To assess



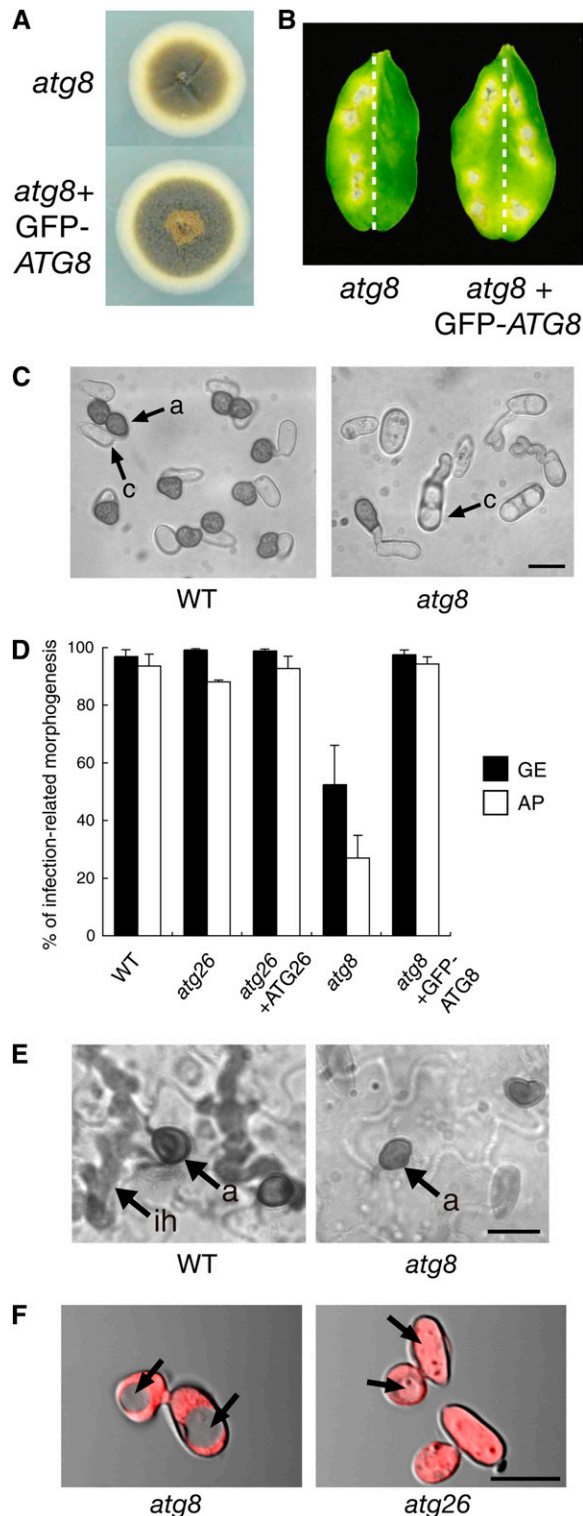


**Figure 8.** Atg8-Dependent Nonselective Autophagy in *C. orbiculare*.

**(A)** The colony phenotype of the *atg8* mutant of *C. orbiculare*. The tested strains were incubated on PDA for 1 week.

**(B)** *ATG8* is required for the fungal pathogenicity of *C. orbiculare*. Conidial suspensions of the tested strain were inoculated onto the right

appressorial turgor, we used a cytorrhysis assay, which measures the number of collapsed appressoria after exposure to varying concentrations of glycerol (Howard et al., 1991; Tanaka et al., 2007). Surprisingly, the *atg26* appressoria tended to collapse less frequently than the wild-type appressoria (Figure 9D). Furthermore, the full length of Co *ATG26* rescued this appressorial phenotype under glycerol treatment in the *atg26* mutant (i.e., the Co *Atg26*-reintroduced transformant showed increased appressorial collapse in the presence of glycerol). By contrast, Co *Atg26* lacking the CAT region (*ATG26*ΔCAT) or Co *Atg26* lacking PBD (*ATG26*ΔPBD) failed to increase the sensitivity of the *atg26* mutant to glycerol, indicating that this appressorial phenotype correlates strongly with the defect in appressorial pexophagy (Figures 9D and 6B). A similar phenotype was also found in the appressoria formed by the *mck1* mutant of *M. oryzae*, defective in the mitogen-activated protein kinase pathway for cell wall integrity (Jeon et al., 2008). These findings suggest that *Atg26*-mediated pexophagy is involved in certain structural aspects of appressorial development, which are subsequently important for efficient host invasion.

## DISCUSSION

In this study, we identified the *C. orbiculare* *Atg26* protein as a pathogenicity factor through the molecular analysis of a non-pathogenic mutant generated by insertional mutagenesis. We first showed that peroxisomes are degraded inside vacuoles during the infection process of wild-type *C. orbiculare*. We then showed that appressoria formed by the *atg26* strain are defective in host invasion. An assay for papillary callose accumulation suggested that *Atg26* is not involved in the development of the penetration peg, a conclusion supported by an *in vitro* invasion assay on nitrocellulose membranes. Furthermore, experiments using FM4-64 showed that the mutants are able to establish a temporal biotrophic phase in the postinvasion stage. These

halves of cucumber cotyledons. We inoculated the wild-type strain (104-T) onto the left halves. The inoculated leaves were incubated for 7 d. **(C)** *ATG8* is involved in the early stage of infection-related morphogenesis. Conidia from the tested strains were incubated on glass for 24 h, a, appressorium; c, conidium. Bar = 10 μm.

**(D)** A quantitative assay of infection-related morphogenesis. Conidia from the tested strains were incubated on glass for 24 h, and their rates of germination (GE) and appressorium formation (AP) were investigated. The germination rate was calculated as the percentage of conidia that germinated, whereas the appressorium formation rate was calculated as the percentage of geminating conidia that formed appressoria. In each experiment, at least 200 conidia were examined. The means and standard deviations were calculated from three independent experiments.

**(E)** Appressoria formed by the *atg8* mutant are nonfunctional. The conidia of the tested strain were inoculated onto cucumber cotyledons and incubated for 4 d. a, appressorium; ih, invasive hypha. Bar = 10 μm.

**(F)** The *atg8* mutant but not the *atg26* mutant has a defect in nonselective autophagy during infection-related morphogenesis. The tested strains were incubated on glass for 24 h. Arrows indicate vacuoles. Bar = 10 μm.

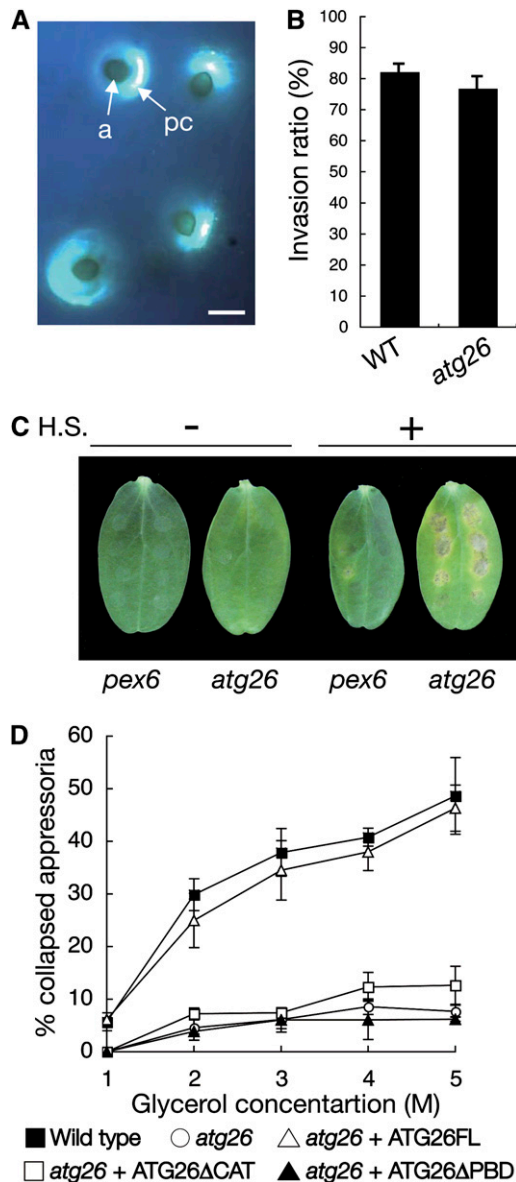


**Figure 9.** Phenotypic Analysis of the *atg26* Mutant in Terms of Its Appressorial Functionality for Host Invasion.

**(A)** Deposition of papillary callose under the appressoria formed by the *atg26* mutant. The *atg26* mutant was inoculated on the nonhost plant *Arabidopsis*. One day after inoculation, the callose deposits in the papillae were stained with aniline blue. a, appressorium; pc, papillary callose deposition. Bar = 10  $\mu$ m.

**(B)** Appressorial penetration assay on nitrocellulose. Conidial suspensions of the *atg26* mutant were inoculated onto nitrocellulose and incubated for two days. In each experiment, at least 200 appressoria were examined to calculate the percentage penetration. Means and standard deviations were calculated from three independent experiments.

**(C)** Pathogenicity of the *atg26* mutant on heat-shocked host plant. Conidial suspensions of the wild-type strain, the *atg26* strain, or the *pex6* strain were inoculated onto heat-shocked (H.S.) cotyledons of cucumber. The inoculated plants were incubated for 1 week.

results indicate a specific function of Atg26 in appressorial functionality for host invasion. Consistent with this, the *atg26* strain exhibited defects in peroxisome degradation in the mature appressorial cells, suggesting the involvement of Atg26 in peroxisome degradation inside appressoria that are developing into the host invasion stage.

The observed pexophagy and phytopathogenicity phenotypes were correlated in studies using several *ATG26* alleles (*atg26*, *atg26* $\Delta$ , and the domain-deleted mutant alleles). Domain deletion analysis of Atg26 suggested that Atg26 requires the PBD as well as its catalytic activity for pexophagy and phytopathogenicity, although we cannot completely exclude the possibility that the three-dimensional structure of the entire Atg26 is crucial in its molecular function.

The introduction of Atg26 without the PBD (*ATG26* $\Delta$ PBD) increased the sterol glucosyltransferase activity of the *atg26* mutant to a level similar to that afforded by full-length Atg26 (*ATG26*FL), but failed to restore the defects of the *atg26* mutant. Furthermore, GFP-based localization analysis of Atg26 suggested that Co Atg26 localizes in putative preautophagosomal structures via its PBD, which is required for fungal pathogenicity. Consistent with these findings, when Pp Atg26 lacking the PBD was expressed under a strong promoter in the Pp *atg26* $\Delta$  mutant of *P. pastoris*, its expression resulted in the synthesis of sterol glucoside beyond the wild-type level, but failed to restore pexophagy, indicating that the total sterol glucoside level does not correlate directly with pexophagy (Oku et al., 2003).

Why is pexophagy necessary for the pathogenicity of *C. orbiculare*? Co Atg26-dependent pexophagy functions in recycling cellular components, including amino acids inside the appressoria, which might promote the protein synthesis required for host invasion. Alternatively, undegraded peroxisomes might have negative effects on the metabolic or structural aspects of appressorium-mediated invasion. The requirement for protein synthesis in the infection strategy of *C. orbiculare* is supported by (1) the inhibition of invasive hyphae formation by cycloheximide (Suzuki et al., 1982) and (2) the involvement of a tRNA methylase (Aph1) in the invasion step (Takano et al., 2006).

Our cytorrhysis assay showed that the appressoria formed by the *atg26* mutant collapsed less frequently with glycerol treatment than did the appressoria of the wild type. This suggests that Atg26 contributes to the cellular integrity of the appressoria in *C. orbiculare*. A mutant of *Fusarium oxysporum* defective in a class V chitin synthase lost its pathogenicity on the host plant tomato (*Solanum lycopersicum*), and its sensitivity to plant antimicrobial defense compounds increased (Madrid et al., 2003). Therefore, in pathogenesis, the integrity of the cell wall is critical to resist plant defense responses, such as attack by antimicrobial compounds. The *atg26* mutant was able to invade the heat-treated leaves of the host plant, suggesting that the failure of the *atg26* mutant in host invasion is associated with host defense

**(D)** Appressorial cytorrhysis assay. For each glycerol concentration, at least 100 appressoria of the tested strains were observed and the numbers of collapsed appressoria were counted from two independent experiments. Error bars represent SD.

[See online article for color version of this figure.]

responses. Atg26-mediated pexophagy might contribute to cell wall development in the infection structures through organelle recycling.

We showed that Atg8 has functions distinct from those of Atg26 (i.e., nonselective autophagy is required for the morphogenesis of the appressorium, whereas Atg26 is specifically involved in the subsequent invasion step). In contrast with the *atg26* mutant, the autophagy-deficient *atg8* mutant failed to germinate effectively, and the germinating conidia failed to develop into appressoria. This suggests that nonselective autophagy contributes greatly to the morphogenesis of the appressoria. Nonselective autophagy is generally triggered by nutrient starvation and is inhibited by nutrient-rich conditions. Interestingly, the Co *atg8* mutant exhibits a severe defect in conidiation on nutrient-rich medium (PDA) (see Supplemental Table 1 online). This result implies the regulation of nonselective autophagy by other factors related to the morphological development of *C. orbiculare*, in addition to the response to nutrient starvation.

Recent studies have demonstrated that sterol glucoside synthesis in preautophagosomal structures is necessary for the enhancement of pexophagy in *P. pastoris* (Oku et al., 2003; Yamashita et al., 2006; Nazarko et al., 2007b). In *P. pastoris*, the dependence of pexophagy on Pp Atg26 seems to increase with the size of the peroxisomes in *P. pastoris* (Nazarko et al., 2007b). However, TEM analysis of *C. orbiculare* suggested that the size of the detected peroxisomes in the conidia is relatively uniform and is also similar to that of the remaining peroxisomes in the appressoria. Thus, it is likely that peroxisomes of similar sizes are formed during conidiogenesis and are equally subjected to degradation.

During infection-related morphogenesis, the conidia of *C. orbiculare* metabolize the fatty acids stored in lipid bodies through  $\beta$ -oxidation within peroxisomes. The functional analysis of *ICL1* (encoding isocitrate lyase) suggested that the peroxisomal glyoxylate cycle is essential for vegetative growth on fatty acids but is dispensable for appressorial melanization of *C. orbiculare* (Asakura et al., 2006). Therefore, acetyl-CoA that is generated appears to be directly used in the appressorium maturation step, such as for melanin biosynthesis (Kimura et al., 2001; Asakura et al., 2006). In the peroxisome assembly mutant *pex6*, these metabolic deficiencies are assumed to lead to impaired appressorium maturation and cause a loss of phytopathogenicity. If peroxisomes are excessively degraded during the early stage of infection, appressorium maturation might be inhibited. Therefore, peroxisome homeostasis must be strictly regulated during this stage. Atg26 may be involved in the regulation of pexophagy efficiency by removing redundant peroxisomes in the mature appressoria.

This study, together with our previous work, demonstrates the physiological importance of peroxisome homeostasis, including both peroxisome assembly and degradation (pexophagy), in the phytopathogenicity of this infectious fungus. Studies of the peroxisome homeostasis of this pathogenic fungus will provide further insight into the role of organellar homeostasis during various cellular functions, and this is likely to reveal highly regulated mechanisms during the development and differentiation processes of higher organisms.

## METHODS

### Fungal Strains, Media, Transformation, and DNA Analysis

*Colletotrichum orbiculare* (syn. *C. lagenarium*) strain 104-T (MAFF240422) was used as the wild-type strain. The *C. orbiculare* strains used in this study are listed in Supplemental Table 2 online. All *C. orbiculare* strains were maintained on 3.9% (w/v) PDA (Difco Laboratories) at 24°C. REMI mutagenesis and the transformation of *C. orbiculare* have all been described previously (Kimura et al., 2001). Restriction enzyme digestion, cloning, plasmid isolation, and gel electrophoresis were performed according to the manufacturers' instructions and standard methods (Sambrook et al., 1989).

### Plasmid Constructs

Co *ATG26* and Co *ATG8* were mutated using an adaptation of a previously described in vitro transposon tagging procedure (Hamer et al., 2001). To mutate Co *ATG26*, a cosmid clone (from the *C. orbiculare* cosmid genomic library in our laboratory), pCOATG26, containing Co *ATG26* was used as the target. Gene disruption vector, pKOATG26, was constructed by mobilizing a modified Tn7 transposable element containing the hygromycin phosphotransferase gene (*HPH*) cassette (Sweigard et al., 1997; Hamer et al., 2001) into pCOATG26 in vitro. The transposon was inserted into Co *ATG26* at nucleotide 1150 (amino acid residue 345) in pKOATG26. The gene disruption vector, pKOATG8, was constructed by mobilizing a Tn7 transposable element containing the *HPH* cassette and the chloramphenicol resistance gene (Sweigard et al., 1997; Hamer et al., 2001; Foster et al., 2003) into pCOATG8 in vitro. The transposon was inserted into the Co *ATG8* sequence between nucleotides 111 and 112 (inside the first intron) in pKOATG8.

For the domain analysis of Co Atg26, the entire Co *ATG26* ORF (amino acids 1 to 1475) was amplified by PCR using the primers 26GS1 and 26GAS1 (see Supplemental Table 3 online). pBATP was constructed previously by the introduction of both the short promoter and terminator regions of the melanin biosynthesis gene *SCD1* into pCB1531 (Sweigard et al., 1997; Kimura et al., 2001). The amplified fragment was digested with *Xba*I and *Spe*I and introduced into pBATP to produce pBATG26FL. For the construction of Co Atg26 lacking the catalytic region, a truncated Co Atg26 was amplified with primers 26GS1 and 26GRD1. The amplified fragment was digested with *Xba*I and *Spe*I and introduced into pBATP to produce pBATG26 $\Delta$ CAT. To construct Co Atg26 lacking its PBD, part of the genomic region of Co Atg26 (nucleotides 864 to 1475), amplified with primers 26GS2 and 26GAS1, was digested with *Xba*I and *Spe*I and introduced into pBATP to produce pBATG26C. A truncated Co Atg26 (nucleotides 1 to 266), amplified with primers 26GS1 and 26GAS2, was digested with *Xba*I and introduced into pBATG26C to produce pBATG26 $\Delta$ PBD. The catalytic region of Co Atg26 (nucleotides 921 to 1475), amplified with primers 26CAS1 and 26GAS1, was also digested with *Xba*I and *Spe*I and introduced into pBATP to produce pBATG26CAT.

For the transformation experiments using geneticin (Sigma-Aldrich) as the selective agent, we transferred each gene cassette of Co *ATG26*, including the short promoter and terminator regions of *SCD1*, into pII99 carrying a geneticin resistance gene (Namiki et al., 2001). The gene cassettes released from pBATG26FL, pBATG26 $\Delta$ CAT, pBATG26 $\Delta$ PBD, and pBATG26CAT were introduced into pII99, which resulted in pIIATG26FL, pIIATG26 $\Delta$ CAT, pIIATG26 $\Delta$ PBD, and pIIATG26CAT, respectively.

To construct the expression vector for the GFP-Co*ATG8* fusion gene (pCB16GFPATG8), the entire *ATG8* ORF was amplified with the primers AT8FSB and AT8FASE (see Supplemental Table 3 online). The amplified fragment was digested with *Eco*RI and *Bam*HI and introduced into pCB16EGFPSPST (Asakura et al., 2006) to produce pCB16GFPATG8.

To analyze the PBD-dependent subcellular localization of Co Atg26, pHGFPATG26FL carrying the *GFP-CoATG26* gene and pHGFPATG26ΔPBD carrying *GFP-CoATG26* lacking the PBD were constructed. The expression of the *GFP-CoATG26* fusion genes was controlled by the short promoter region of *SCD1*. The Co *ATG26* ORF sequence contains one *EcoRI* site. For pHGFPATG26FL, the truncated Co *ATG26* region containing the *EcoRI* site (nucleotides 1 to 2855) was amplified from pCOSATG26 with the primers ATG26FSB and ATG26asA. For pHGFPATG26ΔPBD, the truncated Co *ATG26* region lacking the PBD was amplified from pIIATG26ΔPBD with primers ATG26FSB and ATG26asA. The amplified products from pCOSATG26 and pIIATG26ΔPBD were digested with *Bam*HI and *Eco*RI and introduced into PCB16EGFPSPST, which resulted in pCBGFAT26FL and pCBGFAT26ΔPBD, respectively. Subsequently, the C-terminal truncated region of Co *ATG26* (nucleotide 2700 to the stop codon) was amplified from pCOSATG26 with the primers ATG26sB and ATG26FASE. The amplified product was digested with *Eco*RI and introduced into pCBGFAT26FL and pCBGFAT26ΔPBD to produce pHGFPATG26FL and pHGFPATG26ΔPBD, respectively. To construct the Co *ATG26* replacement vector pGDATG26, the 2.6-kb fragment containing the 3' flanking region of Co *ATG26* was amplified by PCR with the primers ATG26d3K and ATG26d4. Primer ATG26d3K contains a *Kpn*I site. The amplified fragment was digested with *Kpn*I and introduced into the *Kpn*I site of pCB1636 (Sweigard et al., 1997) containing the *HPH* gene to produce plasmid pCB3ATG26. The 2.4-kb fragment containing the 5' flanking region of Co *ATG26* was amplified by PCR with primers ATG26d1X and ATG26d2B. The primer ATG26d1X contains an *Xba*I site, and the primer ATG26d2B contains a *Bam*HI site. The amplified product was digested with *Xba*I and *Bam*HI and introduced into the *Xba*I-*Bam*HI sites of pCB3ATG26 to produce pGDATG26. To express RFP under the *Aureobasidium pullulans* *TEF* promoter (Vanden Wymelenberg et al., 1997), the *TEF* promoter was amplified from pTEFEGFP using the primers TEFNS1 and TEFAS1 and introduced into pBAT, resulting in pBATTEFP (see Supplemental Table 3 online). The entire ORF of mRFP1 was amplified with the primers MRFPXKZ and MRFPSTOPB (Campbell et al., 2002; Asakura et al., 2006) and introduced into pBATTEFP, resulting in pBATTEFPMR. The plasmids pBAGFPPTS1 (for *GFP-SKL*) and pBATPMRPTS1 (for *RFP-SKL*) used in this study have been described previously (Kimura et al., 2001; Asakura et al., 2006).

### Pathogenicity Assays

For the pathogenicity assay, conidial suspensions ( $5 \times 10^5$  conidia per mL) were drop-inoculated onto detached cotyledons of cucumber (*Cucumis sativus*). For inoculation through wound sites, the conidial suspension was spotted onto sites wounded with a 26G<sub>1/2</sub> needle. To heat shock the plants, detached cucumber cotyledons were dipped into distilled water at 50°C for 30 s. The tested strains were then inoculated onto the heat-treated cotyledons. As a control, cotyledons were dipped into distilled water at 25°C for 30 s before inoculation.

### Assay for Appressorium Formation and Functionality

Infection-related morphogenesis was investigated as described previously (Asakura et al., 2006). The formation of invasion hyphae into nitrocellulose and cucumber cotyledons was investigated as described previously (Asakura et al., 2006). The assay for papilla formation on the nonhost plant *Arabidopsis thaliana* was performed as previously described (Shimada et al., 2006). Appressorial turgor was determined using the cytorrhysis assay described previously (Howard et al., 1991; Tanaka et al., 2007). To assay appressorial development, conidia were incubated on multiwell glass microscope slides (ICN Biomedicals) at 24°C for 48 h. Surplus water was removed and replaced with a 1 to 5 M concentration of

glycerol solution. After 15 min of incubation, the number of collapsed appressoria was counted. This experiment was replicated twice.

### Fluorescence Microscopy

Peroxisomes from *C. orbiculare* cells were labeled by the expression of enhanced GFP fused to SKL (*GFP-SKL*) or mRFP1 fused to SKL (*RFP-SKL*). To visualize their vacuoles, the cells were stained with 5 μg/mL Oregon Green 488 cDFFDA (Hicky et al., 2004). In all experiments for analysis of peroxisome dynamics shown here, the conidia were incubated with 10 μg/mL carpropamid, which inhibits melanin biosynthesis (Asakura et al., 2006), although we confirmed the peroxisome degradation in *C. orbiculare* without carpropamid (see Supplemental Figure 5 online). The fluorescence of RFP, GFP, FM4-64, and cDFFDA was observed under a FluoView FV500 confocal microscope (Olympus Optical) as previously described (Asakura et al., 2006). To observe autophagosomal structures labeled with *GFP-CoAtg8*, a conidial suspension was incubated on glass-bottomed microwell dishes (35 mm Petri dishes and 10 mm microwells; MatTek). Images were captured with an IX70 fluorescence microscope (Olympus) equipped with an XF52 filter set (Omega Optical). To observe EIHM in the interaction between the Co *atg26* mutant and cucumber cells, the invasive hyphae of the Co *atg26* mutant were labeled with constitutively expressed GFP under the *A. pullulans* *TEF* promoter. Plant cell membranes were labeled with FM4-64 (Invitrogen). The conidia of the Co *atg26* strain expressing GFP were inoculated onto the lower surfaces of cucumber cotyledons and incubated for 4 d. Epidermal layers were peeled off and stained with 10 μg/mL FM4-64 for 30 min.

### TEM

Samples were prepared for TEM using freeze substitution fixation according to the procedure of Hoch (1986). Briefly, pieces of cucumber cotyledon ( $\sim 1 \times 1$  mm<sup>2</sup>) were excised from beneath the inoculation sites 24 h after inoculation and then quench-frozen by plunging them into liquid propane cooled by liquid nitrogen using a Reichert KF80 quick-freezing unit (Leica). Conidia suspended in water were spread on agarose membranes and frozen similarly. The specimens were substituted in 2% osmium tetroxide in acetone for 48 to 72 h at -80°C and then embedded in epoxy resin (LUVEAK-812; Nacalai Tesque). Ultrathin sections were cut, stained with uranyl acetate and lead citrate, and examined using TEM (H-7100FA; Hitachi).

### Sterol Glucosyltransferase Activity

Each of the cell homogenate samples, containing 0.5 mg of protein, was centrifuged at 100,000g for 1 h. The pelleted fractions were resuspended in 85 μL of reaction buffer (50 mM Tris-HCl, pH 7.5, 5% [v/v] glycerol, and one tablet of Complete protease inhibitor cocktail [Roche Diagnostics] in 100 mL volume). The samples were mixed with 10 μL of UDP-glucose (3.6 mM in water) and 5 μL of cholesterol (6 mM dissolved in ethanol). The reaction mixture was incubated at 30°C for 3 h. After incubation, the lipid moiety was extracted by the addition of 0.6 mL of chloroform/methanol (2:1) solution, dried by evaporation, resuspended in 20 μL of chloroform, and spotted onto Silica gel 60 F<sub>254</sub> plates (Merck). Thin-layer chromatography was performed in chloroform/methanol (85:15). The plate was baked at 120°C for 10 min after it had been sprayed with 2% methylresorcinol dissolved in 2 N sulfuric acid to visualize the glycolipids.

### Accession Numbers

Sequence data from this article can be found in the GenBank/EMBL data libraries under accession numbers AB365480 (Co *ATG8*), AB365481 (Co

ATG26), D86079 (Co *SCD1*), AF343063 (Co *PEX6*), XM\_001727905 (Nc *ATG26*), AF091397 (Pp *ATG26*), and APU1972 (*TEF1*).

#### Supplemental Data

The following materials are available in the online version of this article.

**Supplemental Figure 1.** The REMI Mutant NP71 of *C. orbiculare*.

**Supplemental Figure 2.** Alignment of the Deduced Amino Acid Sequence of *C. orbiculare* Atg26 with a Putative Atg26 Homolog of the Filamentous Fungus *Neurospora crassa* and *P. pastoris* Atg26.

**Supplemental Figure 3.** Gene Disruption of Co *ATG26*.

**Supplemental Figure 4.** Glucose Did Not Restore Pathogenicity of the *atg26* Mutant.

**Supplemental Figure 5.** Time Lapse Analysis of Peroxisome Degradation in Appressorium.

**Supplemental Figure 6.** Peroxisome Degradation of the *atg26* Mutant during Conidial Germination and Appressorium Differentiation.

**Supplemental Figure 7.** Gene Replacement of Co *ATG26*.

**Supplemental Figure 8.** Identification and Knockout Analysis of Co *ATG8* in *C. orbiculare*.

**Supplemental Figure 9.** Nitrogen Starvation Assay.

**Supplemental Table 1.** Characteristics of the Co *atg26* and Co *atg8* Mutants.

**Supplemental Table 2.** Strains and Plasmids Used in This Study.

**Supplemental Table 3.** Primers Used in This Study.

**Supplemental Methods.**

**Supplemental References.**

#### ACKNOWLEDGMENTS

We thank Takashi Tsuge for providing pII99, Roger Y. Tsien for the mRFP1 gene, and John Andrews for pTEFEGFP. This work was supported in part by Industrial Technology Research Grant Program in '06 from the New Energy and Industrial Technology Development Organization of Japan and a Grant-in-Aid for Scientific Research (20380027) from the Ministry of Education, Culture, Sports, Science, and Technology of Japan (Y.T.) and by a Grant-in-Aid for Scientific Research on Priority Area 523, the Center of Excellence program, from the Ministry of Education, Culture, Sports, Science, and Technology of Japan, and Japan Science and Technology Agency, CREST (Y.S.).

Received May 25, 2008; revised February 15, 2009; accepted March 18, 2009; published April 10, 2009.

#### REFERENCES

- Agrios, G.N.** (2004). Colletotrichum diseases. In Plant Pathology, 5th ed. G.N. Agrios, ed (San Diego, CA: Academic Press), pp 487–498.
- Asakura, M., Okuno, T., and Takano, Y.** (2006). Multiple contributions of peroxisomal metabolic function to fungal pathogenicity in *Colletotrichum lagenarium*. *Appl. Environ. Microbiol.* **72**: 6345–6354.
- Bechinger, C., Giebel, K.F., Schnell, M., Leiderer, P., Deising, H.B., and Bastmeyer, M.** (1999). Optical measurements of invasive forces exerted by appressoria of a plant pathogenic fungus. *Science* **285**: 1896–1899.
- Campbell, R.E., Tour, O., Palmer, A.E., Steinbach, P.A., Baird, G.S., Zacharias, D.A., and Tsien, R.Y.** (2002). A monomeric red fluorescent protein. *Proc. Natl. Acad. Sci. USA* **99**: 7877–7882.
- Cao, Y., and Klionsky, D.J.** (2007). Atg26 is not involved in autophagy-related pathways in *Saccharomyces cerevisiae*. *Autophagy* **3**: 17–20.
- de Jong, J.C., McCormack, B.J., Smirnov, N., and Talbot, N.J.** (1997). Glycerol generates turgor in rice blast. *Nature* **389**: 244–245.
- Desai, M., and Hu, J.** (2008). Light induces peroxisome proliferation in *Arabidopsis* seedlings through the photoreceptor phytochrome A, the transcription factor HY5 homolog, and the peroxisomal protein Peroxin11b. *Plant Physiol.* **19**: 1117–1127.
- Desvergne, B., and Wahli, W.** (1999). Peroxisome proliferator-activated receptors: Nuclear control of metabolism. *Endocr. Rev.* **20**: 649–688.
- Eckert, J.H., and Erdmann, R.** (2003). Peroxisome biogenesis. *Rev. Physiol. Biochem. Pharmacol.* **147**: 75–121.
- Fan, J., Quan, S., Orth, T., Awai, C., Chory, J., and Hu, J.** (2005). The *Arabidopsis* *PEX12* gene is required for peroxisome biogenesis and is essential for development. *Plant Physiol.* **139**: 231–239.
- Farré, J.C., Manjithaya, R., Mathewson, R.D., and Subramani, S.** (2008). PpAtg30 tags peroxisomes for turnover by selective autophagy. *Dev. Cell* **14**: 365–376.
- Farré, J.C., and Subramani, S.** (2004). Peroxisome turnover by micro-pexophagy: An autophagy-related process. *Trends Cell Biol.* **14**: 515–523.
- Foster, A.J., Jenkinson, J.M., and Talbot, N.J.** (2003). Trehalose synthesis and metabolism are required at different stages of plant infection by *Magnaporthe oryzae*. *EMBO J.* **22**: 225–235.
- Fujiki, Y., Okumoto, K., Kinoshita, N., and Ghaedi, K.** (2006). Lessons from peroxisome-deficient Chinese hamster ovary (CHO) cell mutants. *Biochim. Biophys. Acta* **1763**: 1374–1381.
- Gurvitz, A., and Rottensteiner, H.** (2006). The biochemistry of oleate induction: Transcriptional upregulation and peroxisome proliferation. *Biochim. Biophys. Acta* **1763**: 1392–1402.
- Hamer, L., et al.** (2001). Gene discovery and gene function assignment in filamentous fungi. *Proc. Natl. Acad. Sci. USA* **98**: 5110–5115.
- Hicky, P.C., Swift, S.R., Roca, M.G., and Read, N.D.** (2004). Live-cell imaging of filamentous fungi using vital fluorescent dyes and confocal microscopy. *Meth. Microbiol.* **34**: 63–87.
- Hoch, H.C.** (1986). Freeze substitution in fungi. In *Ultrastructure Techniques for Microorganisms*, H.C. Aldrich and W.J. Todd, eds (New York: Plenum Press), pp. 183–212.
- Howard, R.J., Ferrari, M.A., Roach, D.H., and Money, N.P.** (1991). Penetration of hard substrates by a fungus employing enormous turgor pressures. *Proc. Natl. Acad. Sci. USA* **88**: 11281–11284.
- Jeon, J., Goh, J., Yoo, S., Chi, M.H., Choi, J., Rho, H.S., Park, J., Han, S.S., Kim, B.R., Park, S.Y., Kim, S., and Lee, Y.H.** (2008). A putative MAP kinase kinase kinase, *MCK1*, is required for cell wall integrity and pathogenicity of the rice blast fungus, *Magnaporthe oryzae*. *Mol. Plant Microbe Interact.* **21**: 525–534.
- Kankanala, P., Czymmek, K., and Valent, B.** (2007). Roles for rice membrane dynamics and plasmodesmata during biotrophic invasion by the blast fungus. *Plant Cell* **19**: 706–724.
- Kim, Y.K., Wang, Y., Liu, Z.M., and Kolattukudy, P.E.** (2002). Identification of a hard surface contact-induced gene in *Colletotrichum gloeosporioides* conidia as a sterol glycosyl transferase, a novel fungal virulence factor. *Plant J.* **30**: 177–187.
- Kimura, A., Takano, Y., Furusawa, I., and Okuno, T.** (2001). Peroxisomal metabolic function is required for appressorium-mediated plant infection by *Colletotrichum lagenarium*. *Plant Cell* **13**: 1945–1957.
- Klionsky, D.J., and Ohsumi, Y.** (1999). Vacuolar import of proteins and organelles from the cytoplasm. *Annu. Rev. Cell Dev. Biol.* **15**: 1–32.
- Kubo, Y., and Furusawa, I.** (1991). Melanin biosynthesis: Prerequisite for successful invasion of the plant host by appressoria of *Colletotrichum*

- and *Pyricularia*. In *The Fungal Spore and Disease Initiation in Plants and Animals*, G.T. Cole and H.C. Hoch, eds (New York: Plenum Publishing), pp. 205–217.
- Liu, X.H., Lu, J.P., Zhang, L., Dong, B., Min, H., and Lin, F.C.** (2007). Involvement of a *Magnaporthe grisea* serine/threonine kinase gene, *MgATG1*, in appressorium turgor and pathogenesis. *Eukaryot. Cell* **6**: 997–1005.
- Madrid, M.P., Di Pietro, A., and Roncero, M.I.** (2003). Class V chitin synthase determines pathogenesis in the vascular wilt fungus *Fusarium oxysporum* and mediates resistance to plant defence compounds. *Mol. Microbiol.* **47**: 257–266.
- Mukaiyama, H., Oku, M., Baba, M., Samizo, T., Hammond, A.T., Glick, B.S., Kato, N., and Sakai, Y.** (2002). Paz2 and 13 other PAZ gene products regulate vacuolar engulfment of peroxisomes during micropexophagy. *Genes Cells* **7**: 75–90.
- Namiki, F., Matsunaga, M., Okuda, M., Inoue, I., Nishi, K., Fujita, Y., and Tsuge, T.** (2001). Mutation of an arginine biosynthesis gene causes reduced pathogenicity in *Fusarium oxysporum* f. sp. *melonis*. *Mol. Plant Microbe Interact.* **14**: 580–584.
- Nazarko, T., Farré, J.C., Polupanov, A.S., Sibirny, A.A., and Subramani, S.** (2007a). Autophagy-related pathways and specific role of sterol glucoside in yeasts. *Autophagy* **3**: 263–265.
- Nazarko, T., Polupanov, A.S., Manjithaya, R.R., Subramani, S., and Sibirny, A.A.** (2007b). The requirement of sterol glucoside for pexophagy in yeast is dependent on the species and nature of peroxisome inducers. *Mol. Biol. Cell* **18**: 106–118.
- Ohsumi, Y.** (2001). Molecular dissection of autophagy: Two ubiquitin-like systems. *Nat. Rev. Mol. Cell Biol.* **2**: 211–216.
- Oku, M., Warnecke, D., Noda, T., Muller, F., Heinz, E., Mukaiyama, H., Kato, N., and Sakai, Y.** (2003). Peroxisome degradation requires catalytically active sterol glucosyltransferase with a GRAM domain. *EMBO J.* **22**: 3231–3241.
- Perfect, S.E., Hughes, H.B., O'Connell, R.J., and Green, J.R.** (1999). *Colletotrichum*: A model genus for studies on pathology and fungal-plant interactions. *Fungal Genet. Biol.* **27**: 186–198.
- Ramos-Pamplona, M., and Naqvi, N.I.** (2006). Host invasion during rice-blast disease requires carnitine-dependent transport of peroxisomal acetyl-CoA. *Mol. Microbiol.* **61**: 61–75.
- Sakai, Y., Oku, M., van der Klei, I.J., and Kiel, J.A.** (2006). Pexophagy: Autophagic degradation of peroxisomes. *Biochim. Biophys. Acta* **1763**: 1767–1775.
- Sambrook, J., Fritsch, E.F., and Maniatis, T.** (1989). *Molecular Cloning: A Laboratory Manual* (Cold Spring Harbor, NY: Cold Spring Harbor Laboratory Press).
- Shimada, C., Lipka, V., O'Connell, R., Okuno, T., Schulze-Lefert, P., and Takano, Y.** (2006). Nonhost resistance in *Arabidopsis-Colletotrichum* interactions acts at the cell periphery and requires action filament functions. *Mol. Plant Microbe Interact.* **19**: 270–279.
- Stromhaug, P.E., Bevan, A., and Dunn, W.A., Jr.** (2001). *GSA11* encodes a unique 208-kDa protein required for pexophagy and autophagy in *Pichia pastoris*. *J. Biol. Chem.* **276**: 42422–42435.
- Subramani, S.** (1993). Protein import into peroxisomes and biogenesis of the organelle. *Annu. Rev. Cell Biol.* **9**: 445–478.
- Suzuki, K., Furusawa, I., Ishida, N., and Yamamoto, M.** (1982). Chemical dissolution of cellulose membranes as a prerequisite for penetration from appressoria of *Colletotrichum lagenarium*. *J. Gen. Microbiol.* **128**: 1035–1039.
- Sweigard, J., Chumley, F., Carrol, A., Farrall, L., and Valent, B.** (1997). A series of vectors for fungal transformation. *Fungal Genet. Newsl.* **44**: 52–55.
- Takano, Y., Takayanagi, N., Hori, H., Ikeuchi, Y., Suzuki, T., Kimura, A., and Okuno, T.** (2006). A gene involved in modifying transfer RNA is required for fungal pathogenicity and stress tolerance of *Colletotrichum lagenarium*. *Mol. Microbiol.* **60**: 81–92.
- Tanaka, S., Yamada, K., Yabumoto, K., Fujii, S., Huser, A., Tsuji, G., Koga, H., Dohi, K., Mori, M., Shiraishi, T., O'Connell, R., and Kubo, Y.** (2007). *Saccharomyces cerevisiae SSD1* orthologues are essential for host infection by the ascomycete plant pathogens *Colletotrichum lagenarium* and *Magnaporthe grisea*. *Mol. Microbiol.* **64**: 1332–1349.
- Vanden Wymelenberg, A.J., Cullen, D., Spear, R.N., Schoenike, B., and Andrews, J.H.** (1997). Expression of green fluorescent protein in *Aureobasidium pullulans* and quantification of the fungus on leaf surfaces. *Biotechniques* **23**: 686–690.
- Veneault-Fourrey, C., Baroah, M., Egan, M., Wakley, G., and Talbot, N.J.** (2006). Autophagic fungal cell death is necessary for infection by the rice blast fungus. *Science* **312**: 580–583.
- Wang, Z.Y., Soanes, D.M., Kershaw, M.J., and Talbot, N.J.** (2007). Functional analysis of lipid metabolism in *Magnaporthe grisea* reveals a requirement for peroxisomal fatty acid beta-oxidation during appressorium-mediated plant infection. *Mol. Plant Microbe Interact.* **20**: 475–491.
- Yamashita, S., Oku, M., Wasada, Y., Ano, Y., and Sakai, Y.** (2006). PI4P-signaling pathway for the synthesis of a nascent membrane structure in selective autophagy. *J. Cell Biol.* **173**: 709–717.